Deep Neural Networks for Black Hole Imaging

Johanna S. Karras, He Sun, Katherine L. Bouman California Institute of Technology

jkarras@caltech.edu, hesun@caltech.edu, klbouman@caltech.edu

1. Introduction

Very long baseline interferometry (VLBI) is a form of radio interferometry that uses an array of physically disconnected telescopes to image astronomical objects at a higher resolution. For instance, the Event Horizon Telescope (EHT) VLBI array recently captured the first image of a black hole shadow in the galaxy M87 [1][3]. A state-of-the-art approach for VLBI imaging is the regularized maximum likelihood (RML) method, which solves for an image that jointly maximizes the measured data log-likelihood and an image regularizer. However, the empirical choice of regularization bias the reconstructed images.

We propose an alternative, data-driven approach that uses a convolutional neural network to reconstruct the hidden image from measurement data. We implement both RML and deep learning methods for VLBI imaging and compare the resulting reconstructed image qualities and their robustness to noise. We also compare each methods' robustness to different types of noise. To our knowledge, this is the first in-depth exploration of deep neural network-based imaging for black hole shadows.

2. Background

2.1. Complex Visibilities

In VLBI imaging, we recover a hidden astronomical image using measurements taken between pairs of telescopes, known as complex visibilities. Each visibility corresponds to a frequency component of the brightness distribution of the object being observed, which depends on the locations of the pair of telescopes \boldsymbol{x} and \boldsymbol{y} and the Earth's rotation at time t. As such, a visibility is given by

$$V_{x,y,t} = g_x g_y e^{[-i(\phi_{x,t} - \phi_{y,t})]} F_{x,y,t} X + n_{x,y,t}$$
 (1)

where $F_{x,y,t}X$ is the frequency component of image X between telescopes x and y at time t. The complex visibility measurement is also influenced by several types of noise, including thermal noise $(n_{x,y,t})$, phase errors $(\phi_{x,t}$ and $\phi_{y,t})$, and telescope amplitude gain errors $(g_x$ and $g_y)$. In this work, we consider thermal noise and amplitude gain errors, but leave phase errors for future work.

2.2. Regularized Maximum Likelihood

The RML method recovers an image by jointly minimizing the loss between (1) the true visibilities and the visibili-

ties of the reconstructed image and (2) pre-defined regularization functions of the reconstructed image.

$$\hat{x} = \underset{x}{\operatorname{arg \, min}} \quad [\chi^2(y, f(x)) + \beta \mathcal{R}(x)] \tag{2}$$

Where \hat{x} is the reconstructed image, $\chi^2(y, f(x))$ is the distance measure between the array of measured visibilities y and visibilities f(x) of reconstructed image x, and $\mathcal{R}(x)$ contains the image regularization functions. β is the hand-selected constant coefficient that controls the amount of regularization imposed on the reconstructed image.

3. Methods

In this section we describe our neural network-based approach for reconstructing images from complex visibilities. The neural network model architecture is largely inspired by [6] and it consists of a single dense layer and UNet.

3.1. Objective Function

The objective function for training the reconstruction neural network aims to minimize the summation of the mean absolute error (MAE) between the true and reconstructed images and the χ^2 between the true and predicted visibilities.

$$\theta^* = \underset{\theta}{\operatorname{arg \, min}} \, \operatorname{MAE}(x, A_{\theta}(y)) + \chi^2(f(A_{\theta}(y)), y) \quad (3)$$

where θ^* represents optimal network parameters, $A_{\theta}(\cdot)$ is the neural network model parametized by θ , x is the true image, y is the measured visibilities, and $f(A_{\theta}(y))$ is the visibilities of the reconstructed image.

3.2. Training and Testing Data

The training data for the neural network are generated entirely based on "Fashion MNIST" dataset images, in order to prevent overfitting to black hole-like images [7]. Our training set consists of 7000 original "Fashion MNIST" images and 7000 data-augmented "Fashion MNIST" images, where augmented images are derived using zoom-out, warp, and rotation in order to increase the diversity of the training set and thereby prevent overfitting. The model is validated on 3000 images from the "Digits MNIST" dataset and another 3000 data-augmented "Fashion MNIST" images [4].

The synthetic VLBI visibility measurements of images are simulated using the ehtim library [2] according to the

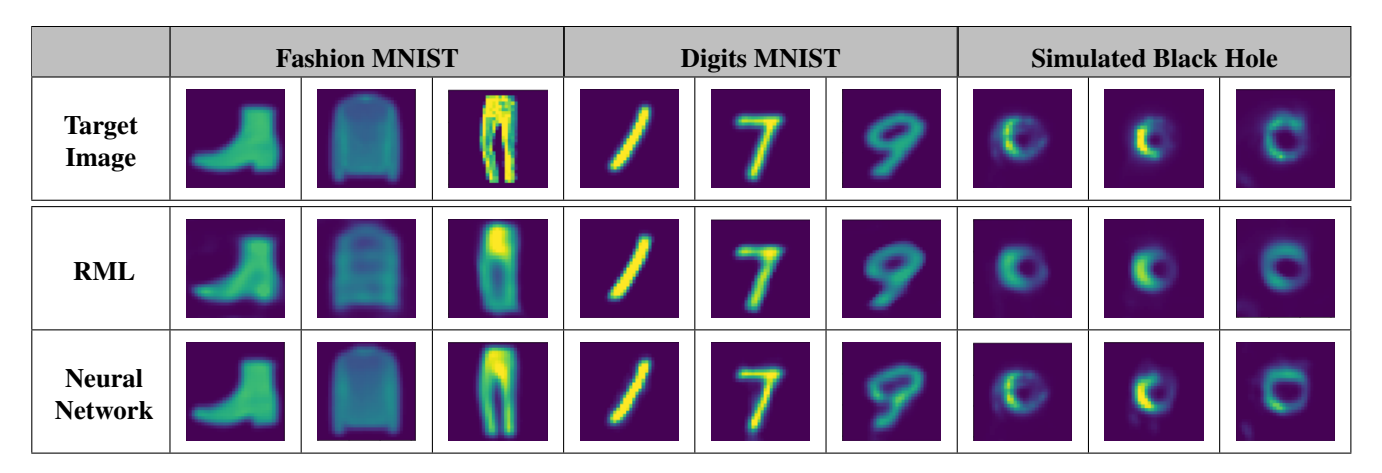


Table 1: Reconstructed images from three different data sets and two different reconstruction methods: (1) RML and (2) a neural network trained with data generated from "Fashion MNIST" images with thermal noise in the measurements. Note that images in a column share the same color bar. Neural network reconstructed images are higher quality for both in-sample (Fashion MNIST) and out-of-sample (Simulated Black Hole) images.

	Fashion MNIST		Digits MNIST		Simulated Black Hole	
	No Noise	Th. Noise	No Noise	Th. Noise	No Noise	Th. Noise
RML	1.396e-4	1.463e-4	1.554e-4	1.623e-4	1.898e-4	2.024e-4
Neural Network w/ No Noise	4.320e-5	4.528e-5	1.036e-4	1.042e-4	1.196e-4	1.201e-4
Neural Network w/ Th. Noise	2.046e-5	3.304e-5	4.957e-5	5.032e-5	1.010e-4	1.012e-4

Table 2: Averaged MAE values for RML and two neural network models, one trained with no noise and another with thermal noise in the training measurements. The results are averaged over 100 different test images from three different datasets. Each dataset was tested using measurements generated with and without random thermal noise in the measurements. Neural network reconstructions achieve lower average MAE for in-sample (Fashion MNIST) and out-of-sample (Simulated Black Hole) images than RML reconstructions.

EHT array configuration in 2019 [3]. The simulated training and testing images are simulated to be 100- μ arcseconds in size, with a flux of 1 Janksy, and at the location of our galactic center black hole Sagittarius A^* .

We test both methods on the training and validation sets, "Fashion MNIST" and "Digits MNIST", as well as an out-of-sample dataset of simulated black hole images [5].

4. Experiments

In the following experiments, we compare RML and our proposed neural network method on various image datasets. We evaluate the quality of reconstructions based on the mean absolute error (MAE) between the true and reconstructed images. Then, we evaluate RML and neural network methods for robustness to thermal noise. We have also considered the effect of adding amplitude gain errors, but due to space considerations do not include those results in this extended abstract.

4.1. Reconstruction Quality

In Table 1, we show that both the RML method and neural network trained with thermal noise produce reasonable images for input visibilities generated from three different image distributions without noise. We also demonstrate that the neural network-reconstructed images are higher resolution and capture more details of the target images. Table 2 quantitatively shows that the average MAE of images reconstructed by the neural networks are lower that the average MAE of images reconstructed by RML across all three datasets.

4.2. Effect of Thermal Noise

Next, we proceed to investigate the methods for robustness to thermal noise. We compare the average performance across 100 images from each dataset of RML, a neural network trained without noise, and a neural network trained with thermal noise in Table 2. The results indicated that both neural networks methods produce reconstructions that achieve lower MAE on average than RML. Of the three reconstruction methods, the neural network trained with thermal noise achieves best performance, since it has the lowest MAE when measurement noise is included.

5. Discussion

In this extended abstract, we began to explore the capabilities of using deep learning for VLBI imaging with complex visibility measurements. We compared this neural network-based approach to the RML method and showed that on average, neural networks reconstruct higher-quality images with a lower MAE than RML for both in-sample and out-of-sample datasets. Additionally, we analyzed both methods with thermal noise added to the measurements and demonstrated that the neural network approach is more robust, even when no noise is incorporated into the training data.

References

- George W Swenson Jr A Richard Thompson, James M Moran. *Interferometry and synthesis in radio astronomy*. Springer Nature. 2017.
- [2] Andrew A. Chael, Michael D. Johnson, Katherine L. Bouman, Lindy L. Blackburn, Kazunori Akiyama, and Ramesh Narayan. Interferometric Imaging Directly with Closure Phases and Closure Amplitudes., 857(1):23, Apr. 2018.
- [3] The Event Horizon Telescope Collaboration. First m87 event horizon telescope results. iv. imaging the central supermassive black hole. 2019.
- [4] Yann LeCun and Corinna Cortes. MNIST handwritten digit database. 2010.
- [5] H. Shiokawa. General-relativistic magnetohydrodynamics simulations of black hole accretion disks: Dynamics and radiative properties. PhD thesis, University of Illinois at Urbana-Champaign, 2013.
- [6] He Sun, Adrian V. Dalca, and Katherine L. Bouman. Learning a probabilistic strategy for computational imaging sensor selection, 2020.
- [7] Han Xiao, Kashif Rasul, and Roland Vollgraf. Fashion-mnist: a novel image dataset for benchmarking machine learning algorithms, 2017.